

BITLIS EREN ÜNIVERSITESI FEN BILIMLERI DERGISI



ISSN: 2147-3129 / e-ISSN: 2147-3188

Article Type:Research ArticleYear: 2025Received:July 9, 2025Volume: 14Revised:September 17, 2025Issue: 3

 Accepted
 : September 19, 2025
 Pages
 : 1921-1941

 DOI
 : 10.17798/bitlisfen.1738850



INVESTIGATION OF PHYSICAL, MECHANICAL, AND DRILLING MACHINABILITY PROPERTIES OF NANOPARTICLES REINFORCED CARBON/GLASS FIBER HYBRID COMPOSITES

Alper GUNOZ 1, * D, Umut Ozgur OZALTAY 1 D

¹ Mersin University, Mechanical Engineering Department, Mersin, Türkiye

* Corresponding Author: alpergunoz@mersin.edu.tr

ABSTRACT

This study aims to investigate the effects of nanoparticle reinforcement, fiber hybridization, and stacking sequences on the mechanical properties and drilling machinability of composite materials. For this purpose, 12-layered polymer composite plates reinforced with graphene nanoplatelets (GnPs) and boron nitride nanoparticles (BNNPs) were produced using the vacuum bagging method. Carbon fiber (CF), glass fiber (GF), and hybrid fiber (HF) with different stacking sequences were used as reinforcements. The samples were subjected to density and hardness measurements, as well as conventional drilling tests. Drilling operations were carried out on a CNC vertical machining center using Ø6.5 mm drills with point angles of 90°, 110°, and 130°, at a constant spindle speed (1000 rpm) and three different feed rates (200, 600, and 1000 mm/min). The results demonstrated that the neat CF specimen exhibited the highest hardness, whereas the incorporation of nanoparticles reduced hardness, with BNNP-reinforced specimens showing the greatest reduction of about 15%. Drilling machinability was significantly enhanced, as evidenced by the reduction in delamination, and the optimum hole diameter (Ø6.48 mm) was achieved in the GF-based composite reinforced with BNNPs using a 130° drill point angle and a feed rate of 200 mm/min. The effects of GnPs and BNNPs on the drilling machinability of fiber-reinforced composites have been investigated only to a limited extent in the literature, and this study provides new insights. These findings may contribute to improving the quality and efficiency of drilling processes in the aerospace and automotive industries.

Keywords: Hybrid composite material, Nanoparticles, Drilling machinability, Graphene

nanoplatelets (GnPs), Boron nitride nanoparticles (BNNPs).

1 INTRODUCTION

Fiber-reinforced polymer matrix composites are widely used in various engineering applications—particularly in the aerospace, automotive, marine, and defense industries—due to their superior properties such as high specific strength, low density, corrosion resistance, and design flexibility [1]. However, despite these advantages, they still exhibit certain limitations, primarily stemming from the brittle nature of the matrix phase, which results in low toughness and poor impact resistance [2, 3]. To overcome these mechanical drawbacks, numerous studies have recently focused on enhancing the performance of composite materials by incorporating various nanoparticles into the matrix phase [4-7]. Nanostructures such as graphene nanoplatelets (GnPs) and hexagonal boron nitride nanoparticles (BNNPs) have demonstrated promising effects on the composite structure due to their high surface area and excellent mechanical properties when added to the matrix [8, 9]. According to the literature, such nanoparticle reinforcements contribute to matrix toughening, thereby increasing the ductility of the overall composite system [10, 11].

Enhancing the mechanical performance of composite materials can be effectively achieved not only by toughening the matrix phase but also by hybridizing the reinforcing elements and optimizing the stacking sequence in hybrid structures [12, 13]. For instance, in CF/GF hybrid composites, CFs contribute high strength and stiffness, whereas GF enhance the overall toughness of the material due to their relatively ductile behavior. Furthermore, a well-designed stacking sequence of the fibers in the hybrid structure can help confine damage under external loading and provide better control over fracture mechanisms [14].

Composite materials undergo various machining processes during their service life, both for dimensional shaping and joining purposes. Among these, drilling is the most common machining operation. Drilling is a complex mechanical process involving the interaction of multi-component cutting forces [15, 16]. The primary challenge encountered during drilling of composite materials is the deformation occurring at the hole entry and exit regions. Such deformations compromise the structural integrity of the composite and significantly reduce its mechanical strength [17]. Therefore, numerous studies have focused on improving hole quality and minimizing damage formation by investigating various parameters. Karaca [15] examined the effects of drill point angle and feed rate on hole deformation in GF reinforced epoxy composites and reported that increases in both parameters lead to increased deformation. Rajamurugan et al. [18] reported that feed rate and drill diameter are the primary factors affecting deformation, while spindle speed has a limited impact. Sunny et al. [19], demonstrated that high spindle speeds combined with low feed rates reduce delamination and burr formation,

with feed rate having a more dominant influence on such damages. Additionally, studies in the literature have reported measurements and analyses of burr size and have focused on deburring techniques [20-22]. Tsao et al. [23] successfully reduced deformation by applying mechanical support at the hole exit. Anaç et al. [24] investigated the mechanical properties and drilling-induced damages of GF epoxy composites produced by different manufacturing methods; they found that hand lay-up samples exhibited higher tensile strength, while the least delamination occurred in samples produced by 3D printing. Unal [25] studied the effects of drill point angle and process parameters on thrust force and temperature during drilling of GF reinforced composites. The findings revealed that feed rate predominantly affects thrust force, whereas point angle has a stronger influence on temperature. Vankanti et al. [26] explored the effects of cutting speed, feed rate, point angle, and cutting edge width on thrust force during drilling of GF composites, highlighting feed rate as the most influential parameter. Gemi et al. [27] examined the influence of different drill geometries and process parameters on damage formation in GF reinforced composite pipes, demonstrating that drill type and feed rate directly affect hole quality.

Several studies have investigated the effects of nanoparticle reinforcement, hybridization, and stacking sequences on the mechanical properties and drilling machinability of composites. Singh and Kumar [28] demonstrated that the addition of multi-walled carbon nanotubes (MWCNTs) reduces delamination and surface roughness in GF epoxy composites. Similarly, Heidary et al. [29] reported that MWCNTs significantly contribute to the reduction of delamination and thrust force in GF epoxy composites. Sathish and Varadhan [30] found that the incorporation of MWCNTs and nano-SiO₂ considerably decreases delamination in basalt fiber (BF)/GF hybrid composites. Erhan et al. [31] highlighted the importance of stacking sequences on mechanical behavior and hole quality in BF reinforced composite pipes. Patel et al. [32] investigated the effect of stacking sequences on the drilling machinability of BF/GF hybrid composites and reported that stacking sequences significantly influences the results. Gemi et al. [33] experimentally examined the mechanical properties and machinability of filament-wound CF/GF fiber hybrid composites with various stacking sequences. Their results indicated that placing a CF layer between two GF layers yields better mechanical performance and machinability characteristics.

A review of the literature indicates that most investigations on drilling of FRP composites have focused on machining parameters such as feed rate, spindle speed, drill diameter, and drill type in order to improve hole quality. Although some studies have explored the role of nanoparticle additives, such as MWCNTs, and the effect of stacking sequences,

research on the influence of GnPs and BNNPs remains scarce. In particular, no comprehensive study has simultaneously addressed how these reinforcements, in combination with hybridization and stacking sequences, affect drilling-induced damages. Moreover, the correlation between such modifications and the fundamental physical and mechanical properties of the composites has not yet been systematically investigated. Therefore, this study aims to fill this gap by experimentally examining the combined effects of drill point angle, feed rate, GnPs and BNNPs reinforcement, hybridization, and stacking sequences on drilling machinability, while also evaluating density and hardness as key material properties. This integrated approach provides new insights into tailoring both the performance and machinability of advanced hybrid composites.

2 MATERIAL AND METHOD

2.1 Materials

In the present study, a diglycidyl ether of bisphenol A (DGEBA)-based epoxy laminating resin (MGS[®] L285) and its corresponding hardener (MGS[®] H285), both manufactured by Hexion, were utilized. The reinforcing materials consisted of CF fabric (245 g·m⁻², twill weave) and GF fabric (300 g·m⁻², twill weave), procured from Dost Kimya (Istanbul, Turkey). Detailed technical properties of the epoxy resin and hardener system are presented in Table 1. In this study, GnPs (Purity:99.9%, Size: 3 nm, Specific Surface Area: 800 m²·g⁻¹, Diameter: 1.5 μm) and BNNPs (Purity: 99.85+%, Size: 65-75 nm, Hexagonal) supplied by Nanografi Nanotechnology AS (Ankara, Turkey) were incorporated into the epoxy resin.

Table 1. Material properties of the epoxy system used in nanocomposite manufacturing

Property	Epoxy Matrix (L285)	Hardener (H285)
Density	$1.18 - 1.23 \text{ g} \cdot \text{cm}^{-3}$	$0.94 - 0.97 \text{ g} \cdot \text{cm}^{-3}$
Viscosity (25 °C)	600 - 900 mPa·s	50 - 100 mPa·s
Gel time	2 - 3 h at 20 - 25 °C; 45	5-60 min at 40 - 45 °C
Mixing ratios	$100:40 \pm 2$ (by weight); 1	$100:50 \pm 2$ (by volume)

2.2 Composite Fabrication

12-layered CF, GF, and CF/GF epoxy composites, both with and without nanoparticle reinforcements, were fabricated using the vacuum bagging method. The composite manufacturing process is illustrated in Figure 1. For the reinforced samples, the ratios of GnPs (0.25 wt.%) and BNNPs (0.5 wt.%) were selected based on previous studies reported in the

literature [9, 34-37] to ensure effective reinforcement while minimizing agglomeration and processing difficulties. After the nanoparticles were incorporated into the epoxy, the mixture was mechanically stirred for 5 minutes, followed by ultrasonic stirring for 15 minutes using a probe with a diameter of Ø13 mm to ensure uniform dispersion. The ultrasonic device had a nominal power of 200 W and operated at a frequency of 20 kHz. The mixing was performed at 85% amplitude in a pulsed mode with a cycle of 2 s on and 3 s off to limit temperature rise. Temperature was monitored and controlled via a thermocouple built into the device. Subsequently, the hardener was added to the reinforced epoxy and mixed mechanically for an additional 5 minutes to achieve homogeneity. The curing process involved a pre-curing stage at 70 °C for 1 hour, followed by a post-curing stage at 100 °C for 3 hours in an autoclave oven, with heating and cooling rates of approximately 1.5 °C/min.

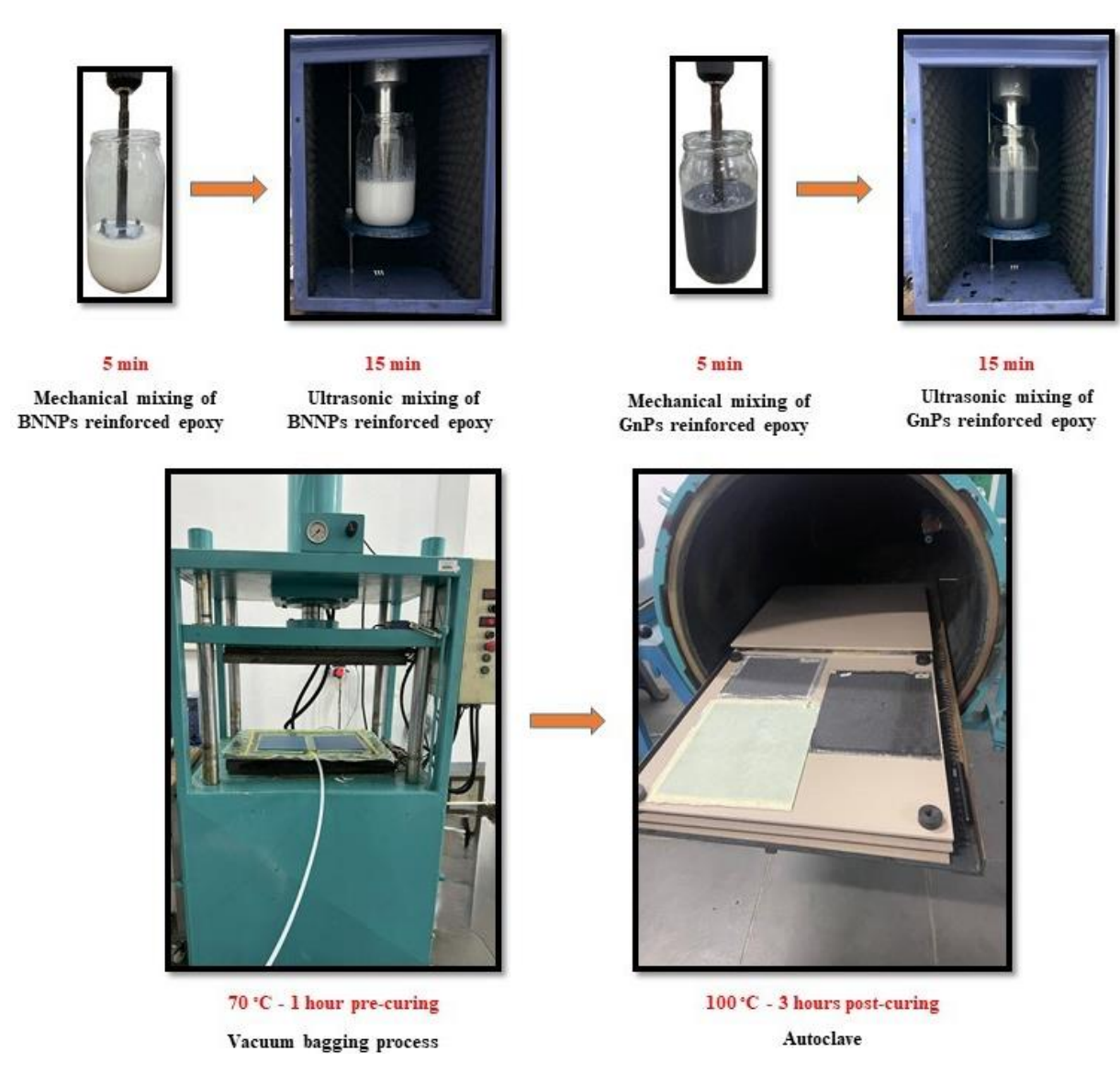


Figure 1. Production process of the composite specimens.

Figure 2 schematically illustrates the stacking sequences of the composite specimens produced in this study. Figures 2a and 2b represent 12-layer composites reinforced solely with CF and GF, respectively. Figures 2c, 2d, and 2e show the HF configurations, labeled as HF1, HF2, and HF3 according to their stacking sequences. The specimens shown in Figures 2f–2j correspond to those in Figures 2a–2e, respectively, with the addition of GnPs into the matrix. Similarly, Figures 2k–2o represent the BNNPs modified versions of the same composites. Figures 2p–2t depict hybrid nanocomposites in which both GnPs and BNNPs were incorporated into the matrix. In total, 20 different composite configurations were fabricated for this study.

The naming of composite specimens begins with the type of reinforcement: "N" denotes neat specimens, "G" indicates GnPs-reinforced, "B" represents BNNPs-reinforced, and "G-B" refers to specimens reinforced with both GnPs and BNNPs. This is followed by the fiber type: "CF" for carbon fiber, "GF" for glass fiber, and "HF1," "HF2," and "HF3" for three different stacking sequences of hybrid fibers. For instance, the designation "G-B-CF" refers to a carbon fiber epoxy composite specimen reinforced with both GnPs and BNNPs. A summary of the sample coding and contents is provided in Table 2 to facilitate comparison of the different composite configurations.

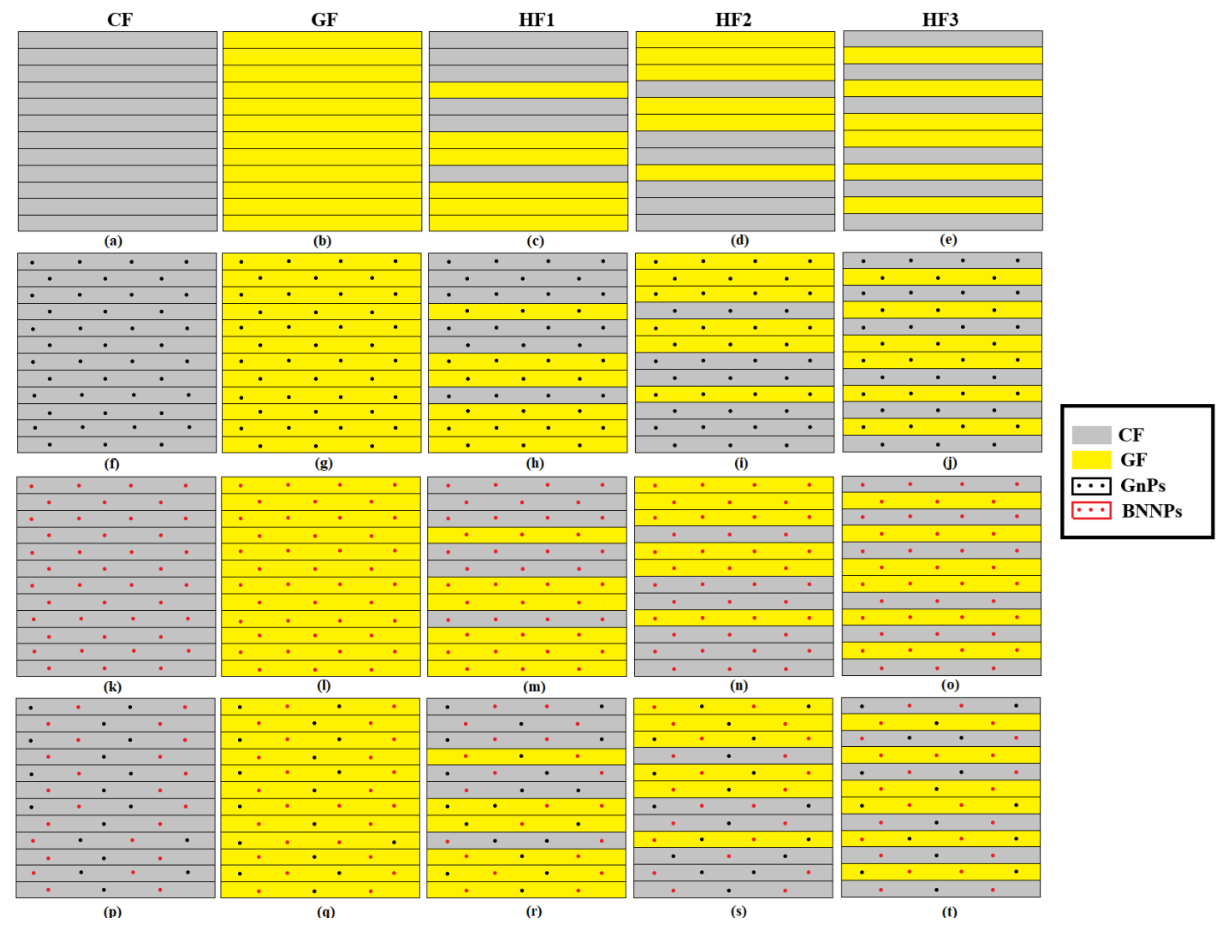


Figure 2. Schematic illustration of the stacking sequences of the composite specimens.

Table 2. Nomenclature of produced composite materials

Sample Code	Sample Content	Stacking Sequence of Layers			
N-CF	Neat carbon fiber epoxy composite	$[CF_{12}]$			
N-GF	Neat glass fiber epoxy composite	$[GF_{12}]$			
N-HF1	Neat hybrid fiber epoxy composite 1	[CF ₃ , GF, CF ₂ , GF ₂ , CF, GF ₃]			
N-HF2	Neat hybrid fiber epoxy composite 2	[GF ₃ , CF, GF ₂ , CF ₂ , GF, CF ₃]			
N-HF3	Neat hybrid fiber epoxy composite 3	[CF, GF, CF, GF, CF, GF] _s			
G-CF	GnPs reinforced carbon fiber epoxy composite	[CF ₁₂]+GnPs			
G-GF	GnPs reinforced glass fiber epoxy composite	[GF ₁₂]+GnPs			
G-HF1	GnPs reinforced hybrid fiber epoxy composite 1	[CF ₃ , GF, CF ₂ , GF ₂ , CF, GF ₃]+GnPs			
G-HF2	GnPs reinforced hybrid fiber epoxy composite 2	[GF ₃ , CF, GF ₂ , CF ₂ , GF, CF ₃]+GnPs			
G-HF3	GnPs reinforced hybrid fiber epoxy composite 3	[CF, GF, CF, GF, CF, GF] _s +GnPs			
B-CF	BNNPs reinforced carbon fiber epoxy composite	[CF ₁₂]+BNNPs			
B-GF	BNNPs reinforced glass fiber epoxy composite	[GF ₁₂]+BNNPs			
B-HF1	BNNPs reinforced hybrid fiber epoxy composite 1	[CF ₃ , GF, CF ₂ , GF ₂ , CF, GF ₃]+BNNPs			
B-HF2	BNNPs reinforced hybrid fiber epoxy composite 2	[GF ₃ , CF, GF ₂ , CF ₂ , GF, CF ₃]+BNNPs			
B-HF3	BNNPs reinforced hybrid fiber epoxy composite 3	[CF, GF, CF, GF, CF, GF] _s +BNNPs			
G-B-CF	GnPs and BNNPs reinforced carbon fiber epoxy composite	[CF ₁₂]+GnPs+BNNPs			
G-B-GF	GnPs and BNNPs reinforced glass fiber epoxy composite	[GF ₁₂]+GnPs+BNNPs			
G-B-HF1	GnPs and BNNPs reinforced hybrid fiber epoxy composite 1	[CF ₃ , GF, CF ₂ , GF ₂ , CF, GF ₃]+GnPs+BNNPs			
G-B-HF2	GnPs and BNNPs reinforced hybrid fiber epoxy composite 2	[GF ₃ , CF, GF ₂ , CF ₂ , GF, CF ₃]+GnPs+BNNPs			
G-B-HF3	GnPs and BNNPs reinforced hybrid fiber epoxy composite 3	[CF, GF, CF, GF, CF, GF] _s +GnPs+BNNPs			

2.3 Density Measurement

The density of the composite specimens was determined based on Archimedes' principle, in accordance with ASTM D792 [38]. Test specimens were cut into 75 mm \times 75 mm squares with a thickness of approximately 3 mm. Although the standard allows for specimens of different shapes and sizes, care was taken to ensure smooth edges and flat surfaces to avoid errors due to compressive stress or frictional heating during cutting. Prior to testing, the surfaces of the specimens were cleaned with compressed air to remove dust and debris, and all specimens were conditioned at 23 \pm 2 °C and 50 \pm 5% relative humidity for 48 h.

Each specimen was first weighed in air (W_{air}) using an analytical balance (DESIS NHB model, Turkey) with a precision of 0.001 g, and then immersed in distilled water at 23 ± 2 °C (ρ_{water} =0.997 g·cm⁻³) and weighed again (W_{water}), as shown in Figures 3(a) and 3(b). Figure 3(a) illustrates weighing the dry specimen, while Figure 3(b) shows the specimen suspended in water. Two measurements were performed for each specimen, and the arithmetic average was calculated. The density (ρ) was calculated using Equation (1).

$$\rho = \frac{W_{air}}{W_{air} - W_{water}} \rho_{water} \tag{1}$$

All test conditions, including water temperature and measurement procedure, were in accordance with ASTM D792 [38]. Care was taken to ensure the specimen was fully immersed

without contact with the vessel walls. The final reported density values represent the average of all measured specimens for each composite configuration.

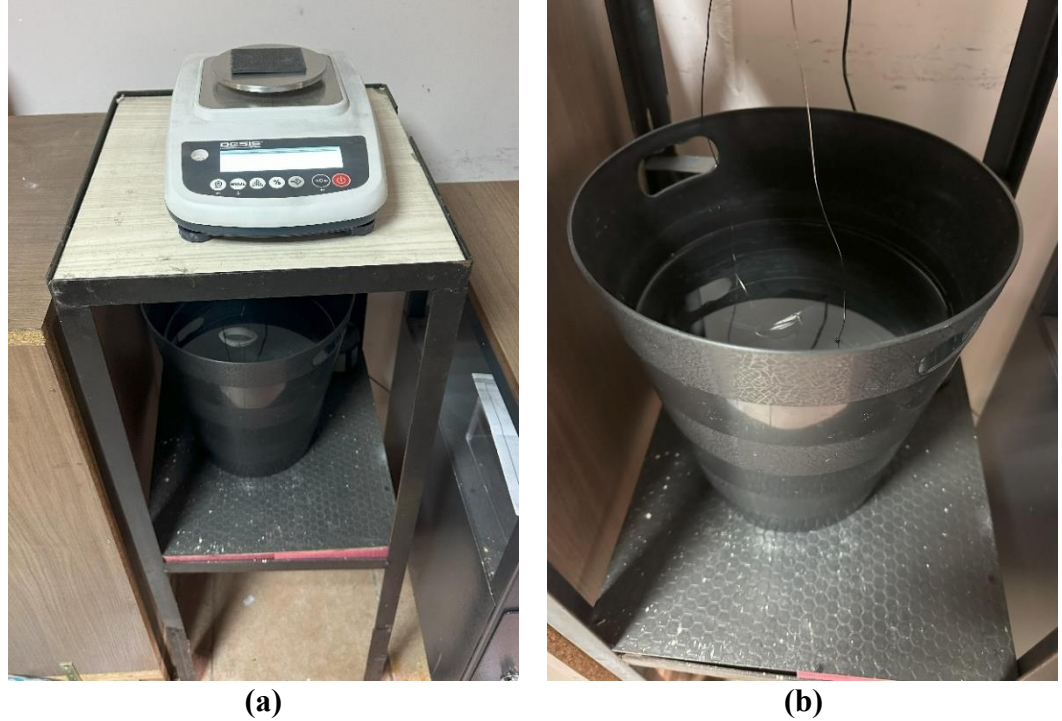


Figure 3. Weighing of composite specimens on a precision balance: (a) dry and (b) wet.

2.4 Hardness Measurement

The hardness of the composite specimens was measured using a Rockwell hardness device (Digirock-RB model, BMS Bulut brand, Turkey), as shown in Figure 4. Test specimens were cut and prepared according to ASTM D785 [39]. Test specimens were cut into 75 mm \times 75 mm squares with a thickness of approximately 3 mm. Although the standard specifies a minimum thickness of 6 mm, ASTM D785 allows the use of thinner specimens if it has been verified that the hardness values are not affected by the supporting surface and that no imprint appears beneath the specimen during testing. The surfaces of the composite specimens were cleaned with compressed air to remove dust and debris. Prior to testing, all specimens were conditioned at 23 ± 2 °C and $50 \pm 5\%$ relative humidity for 48 h.

The measurements were carried out using the Rockwell L scale, which is widely preferred for polymer-based materials. According to this method, a steel ball indenter with a diameter of 6.35 mm was used, applying a minor load of 10 kg and a major load of 60 kg. All tests were conducted at room temperature. Each specimen was placed on a flat and rigid surface, and the indenter was pressed into the material. Hardness values (HRL) were recorded 10 seconds after stable contact was achieved. For each specimen, measurements were taken at six

different locations, and the arithmetic average values were calculated. The Rockwell hardness tester was calibrated according to the standard procedure using appropriate test blocks before measurements to ensure accuracy.



Figure 4. Rockwell hardness test setup for composite specimens (L scale, 6.35 mm steel ball, 10 kg minor load, 60 kg major load)

2.5 Drilling Processes

The drilling operations were performed on composite specimens fixed to a Topper TMV 850A CNC vertical machining center using a vise. High-speed steel (HSS) drill bits with a diameter of Ø6.5 mm and point angles of 90°, 110°, and 130° were employed. Since no official standard exists for drilling-induced damages in polymer composites, the test procedure was adapted from previous studies [40, 41]. The drilling was carried out without pecking or coolant, directly plunging into the material. The spindle speed was kept constant at 1000 rpm, while the feed rates were set at 200, 600, and 1000 mm/min. The spindle speed and feed rates were chosen based on previous studies [42, 43] on polymer composite drilling to represent typical ranges used in similar materials.

The composite specimens were securely clamped on the CNC machine using custom aluminum fixtures, which acted as support plates beneath the specimens. These fixtures prevented deflection of the composite panels during drilling, ensuring consistent hole quality [44]. The aluminum support plates had a thickness of 10 mm and were machined flat to guarantee uniform contact with the specimen surface. Figure 5 shows the composite specimens mounted on the CNC machine and the drill bit point angles used.

Each drilling condition (combination of feed rate and point angle) was repeated on three specimens to ensure reproducibility. Multiple holes were drilled on each specimen, with a minimum spacing of 15 mm to prevent interaction effects. All procedures were performed at room temperature, and the specimens were conditioned under controlled laboratory conditions prior to testing.

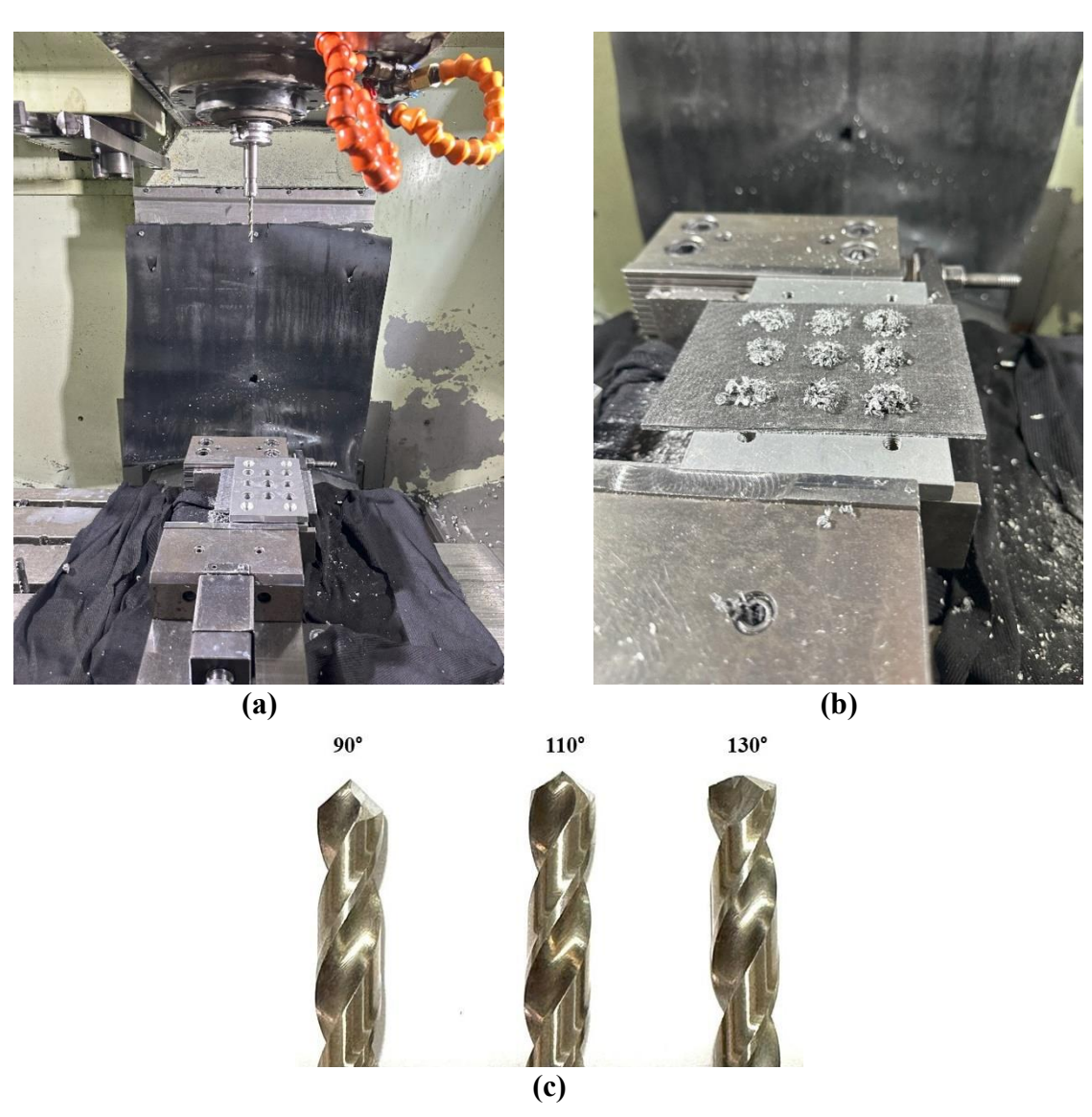


Figure 5. (a) Composite specimen before drilling, (b) composite specimen after drilling, and (c) drill bits with different point angles.

3 RESULTS AND DISCUSSION

3.1 Density Measurement Results

Figure 6 presents the density values of neat and nanoparticle-reinforced composite specimens. Among the neat samples, N-CF, N-GF, N-HF1, N-HF2, and N-HF3 exhibited approximate densities of 1.29, 1.65, 1.59, 1.59, and 1.53 g·cm⁻³, respectively. In this group, the highest density was recorded for the N-GF sample, while the lowest was observed in the N-CF specimen. The lowest density in N-CF can be attributed to the relatively lower areal weight of CF compared to GF (245 g·m⁻² for CF vs. 300 g·m⁻² for GF) and possible void formation during the manufacturing process [45]. The densities of the hybrid-reinforced samples fell between these two extremes.

Upon the addition of nanoparticles (GnPs and/or BNNPs), a general trend of increasing density was observed. This increase can be attributed not only to the higher intrinsic densities of the nanoparticles but also to their good dispersion within the epoxy matrix, which reduces porosity and fills interstitial spaces, as well as the enhanced fiber–matrix interface bonding due to nanoparticle reinforcement. This increase can be attributed not only to the higher intrinsic densities of the nanoparticles but also to their good dispersion within the epoxy matrix, which reduces porosity and fills interstitial spaces, as well as the enhanced fiber–matrix interface bonding due to nanoparticle reinforcement. The highest density values were obtained in the samples reinforced with both GnPs and BNNPs. Among all specimens, the highest density—1.83 g·cm⁻³—was measured for the G-B-GF sample. These observations are consistent with previous studies reporting that well-dispersed nanoparticles improve packing and reduce void content in polymer composites [46, 47].

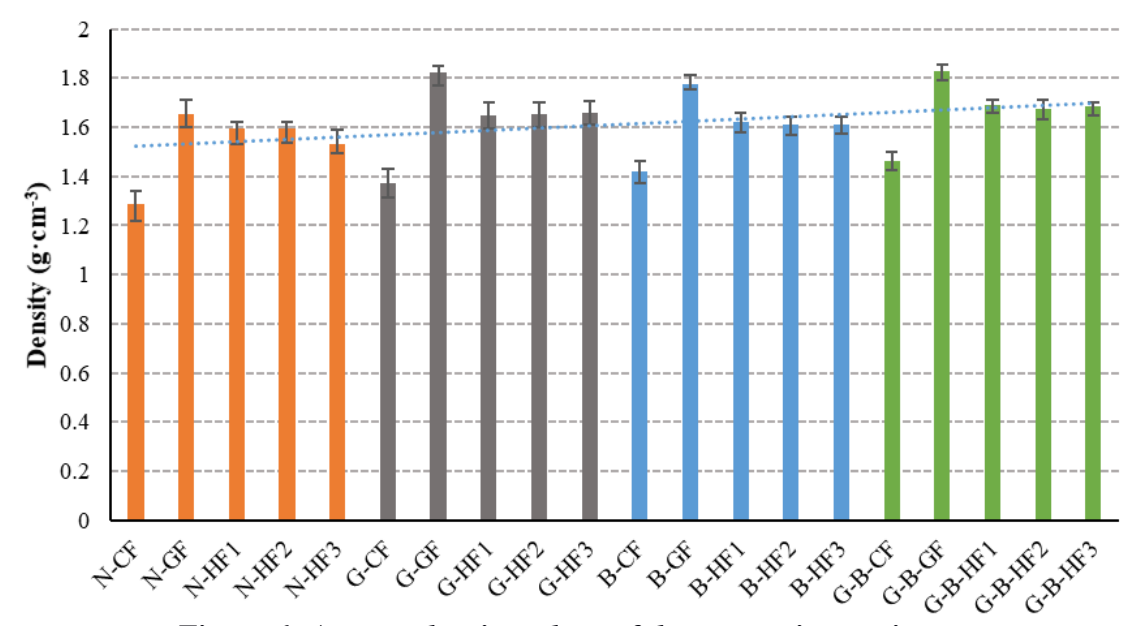


Figure 6. Average density values of the composite specimens.

3.2 Hardness Measurement Results

Figure 7 shows the Rockwell hardness (HRL) values of the neat and nanoparticle-reinforced composite specimens. The average hardness values of the neat specimens N-CF, N-GF, N-HF1, N-HF2, and N-HF3 were measured as 114.95, 88.65, 94.47, 93.53, and 96.68 HRL, respectively. The highest hardness was observed in the N-CF specimen, while the lowest hardness was recorded for the N-GF specimen. This difference is attributed to the more ductile nature of the GF-based composite compared to the CF-based composite. The hardness values of the hybrid-reinforced neat specimens fall between these two extremes.

The incorporation of GnPs and/or BNNPs nanoparticles into the composite structure resulted in a general decrease in hardness, indicating that nanoparticle reinforcement enhances the matrix toughness and improves the composite's ductility [10]. The reduction in hardness can be seen as a positive effect in terms of enhancing toughness-related properties such as impact absorption capacity. Additionally, the differences in hardness between GF- and CF-based composites may not only result from variations in ductility but can also be influenced by other factors, such as the fiber elastic modulus, fiber volume fraction, and fiber/matrix adhesion [48].

Furthermore, BNNPs reinforcement was found to cause a more significant increase in ductility compared to GnPs. Consequently, the lowest hardness values were measured in the BNNPs-containing specimens. Among all samples, the lowest average hardness was found in the B-GF specimen, with a value of 75.35 HRL.

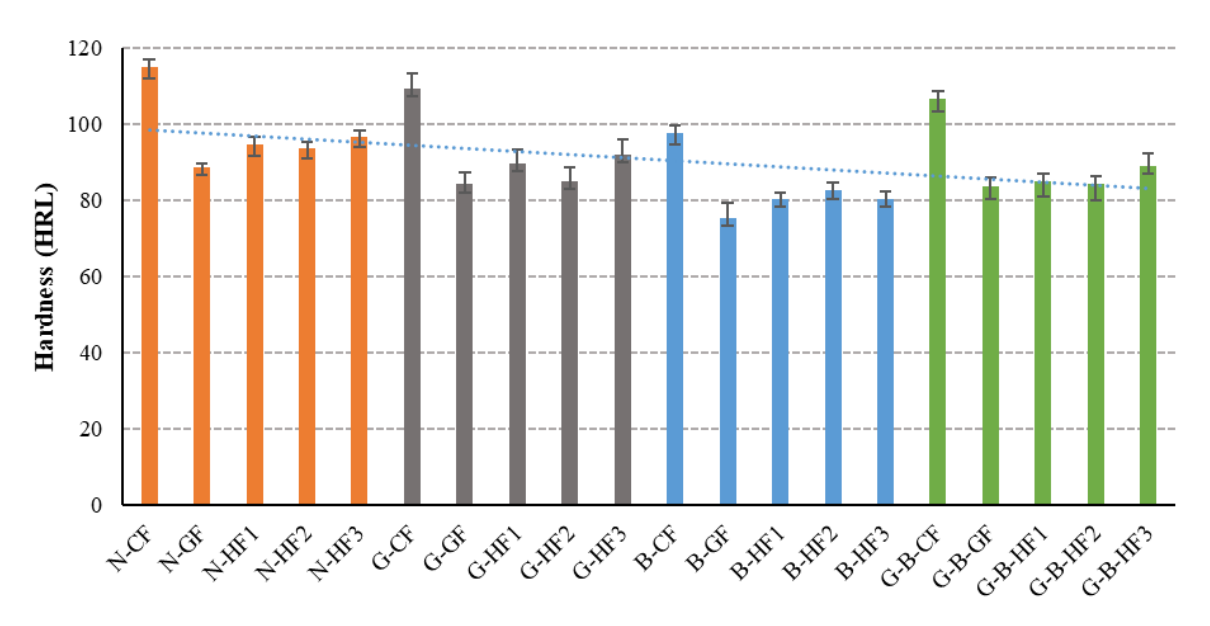


Figure 7. Average hardness values of the composite specimens.

3.3 Drilling Machinability Results

The measured hole diameters as a result of drilling are presented in Table 3. According to Table 3, the hole diameters obtained under all drilling conditions were smaller than the nominal drill diameter. The closest hole diameter to the nominal value (Ø6.48 mm) was measured in the B-GF specimen drilled using a 130° point angle and a feed rate of 200 mm/min. It was observed that increasing the feed rate at a constant point angle resulted in smaller hole diameters, whereas increasing the point angle at a constant feed rate led to larger hole diameters. Feed rate is a critical parameter affecting thrust force, exit delamination, and hole diameter in drilling operations [49]. Notably, a strong linear relationship exists between feed rate and thrust force; as the feed rate increases, the thrust force applied by the tool to the material also increases [50]. According to the literature, thrust force is considered the most influential factor in the formation of delamination. Therefore, reducing the feed rate lowers the thrust force and helps minimize both entrance and exit delamination [51]. On the other hand, higher feed rates may cause excessive heat generation due to friction around the hole, which can locally degrade the polymer matrix and reduce the overall hole quality [52]. It is also important to note that the decrease in hole diameter with increasing feed rate is accompanied by an increase in the delamination factor, which represents the extent of interlaminar separation around the drilled hole. In other words, while higher feed rates tend to produce smaller hole diameters, they also promote more severe damage in terms of delamination [53].

Moreover, under the same point angle and feed rate conditions, larger hole diameters were observed in the nanoparticle-reinforced composites. The observed decrease in hardness due to nanoparticle reinforcement also correlates with the improved drilling machinability, as a more ductile matrix accommodates cutting forces better, reducing delamination and promoting more uniform hole diameters. This can be attributed to the ability of GnPs and BNNPs to make the matrix phase more ductile, thereby facilitating the interaction between the tool and the material. The more ductile matrix structure contributed to more stable cutting conditions during drilling, resulting in improved machinability to some extent. Similar trends have been reported in previous studies. Kaybal et al. [54] demonstrated that the incorporation of BNNPs reduced the delamination factor of CF/epoxy composites, attributing this improvement to the enhanced shear and bending resistance imparted by the BNNPs. Thakur and Singh [55] investigated the effect of different loadings of GnPs on the drilling machinability of GF/epoxy composites, reporting the lowest delamination factor for specimens containing 0.25 wt.% GnPs. This improvement was ascribed to the increased interlaminar bonding strength provided by the

GnPs. Furthermore, Thakur et al. [56] reported that the addition of GnPs formed a bridging network, delayed crack propagation, and improved the fiber–matrix interfacial strength, thereby enhancing the bearing strength and reducing drilling-induced damage in both CF and GF composites. Additionally, due to the relatively more brittle nature of CF compared to GF, crack propagation was more pronounced in CF-based composites.

Table 3. Hole diameters (mm) obtained in composite materials at different point angles and feed rates

	Point Angles (°)- Feed Rates (mm/min)									
Material	90°			110°			130°			
	200	600	1000	200	600	1000	200	600	1000	
N-CF	6.24	6.22	6.20	6.26	6.24	6.22	6.32	6.30	6.26	
N-GF	6.34	6.30	6.28	6.36	6.32	6.30	6.38	6.34	6.32	
N-HF1	6.28	6.26	6.22	6.30	6.28	6.24	6.32	6.30	6.28	
N-HF2	6.30	6.24	6.20	6.32	6.26	6.22	6.38	6.28	6.26	
N-HF3	6.28	6.26	6.22	6.34	6.30	6.26	6.36	6.30	6.28	
G-CF	6.28	6.26	6.24	6.30	6.28	6.26	6.40	6.38	6.28	
G-GF	6.36	6.32	6.30	6.38	6.36	6.34	6.40	6.38	6.36	
G-HF1	6.32	6.28	6.24	6.36	6.30	6.26	6.38	6.32	6.30	
G-HF2	6.34	6.28	6.26	6.44	6.30	6.28	6.46	6.32	6.30	
G-HF3	6.30	6.28	6.24	6.40	6.32	6.28	6.42	6.32	6.30	
B-CF	6.40	6.28	6.26	6.42	6.38	6.32	6.44	6.40	6.36	
B-GF	6.44	6.34	6.32	6.46	6.36	6.34	6.48	6.38	6.36	
B-HF1	6.40	6.34	6.26	6.42	6.36	6.28	6.44	6.38	6.30	
B-HF2	6.38	6.32	6.22	6.40	6.34	6.26	6.46	6.36	6.30	
B-HF3	6.42	6.30	6.24	6.44	6.32	6.28	6.46	6.34	6.30	
G-B-CF	6.38	6.34	6.32	6.40	6.36	6.34	6.42	6.38	6.36	
G-B-GF	6.40	6.36	6.30	6.42	6.38	6.36	6.44	6.40	6.38	
G-B-HF1	6.38	6.34	6.24	6.40	6.36	6.28	6.42	6.38	6.30	
G-B-HF2	6.36	6.32	6.30	6.38	6.34	6.32	6.40	6.36	6.34	
G-B-HF3	6.36	6.30	6.26	6.38	6.36	6.32	6.40	6.38	6.34	

The surface images of the drilled holes obtained from composite specimens under various point angles and feed rates are presented in Figure 8. Examination of Figure 8 reveals that delamination and burr formation increased with increasing feed rate, which is consistent with trends reported in the literature [42]. Davim and Reis [57, 58] stated that delamination tends to increase with cutting parameters such as feed rate and spindle speed. Since the spindle speed was kept constant in this study, the observed increase in delamination and burr formation is directly associated with the increased feed rate.

The most pronounced delamination and burr formation occurred at a point angle of 130° and a feed rate of 1000 mm/min. In contrast, the least burr formation was observed at a feed rate of 200 mm/min. This behavior can be attributed to the lower mechanical loads and thermal effects induced on the material at lower feed rates.

When evaluating the neat and reinforced specimens within their respective groups, it was observed that GF-based composites (N-GF, G-GF, B-GF, G-B-GF) exhibited less delamination and burr formation. This can be explained by the more ductile nature of GF-based specimens, which allows them to better withstand cutting forces and thus exhibit superior machinability. The enhanced ductility helps absorb cutting-induced stresses more effectively, thereby contributing to improved surface integrity.

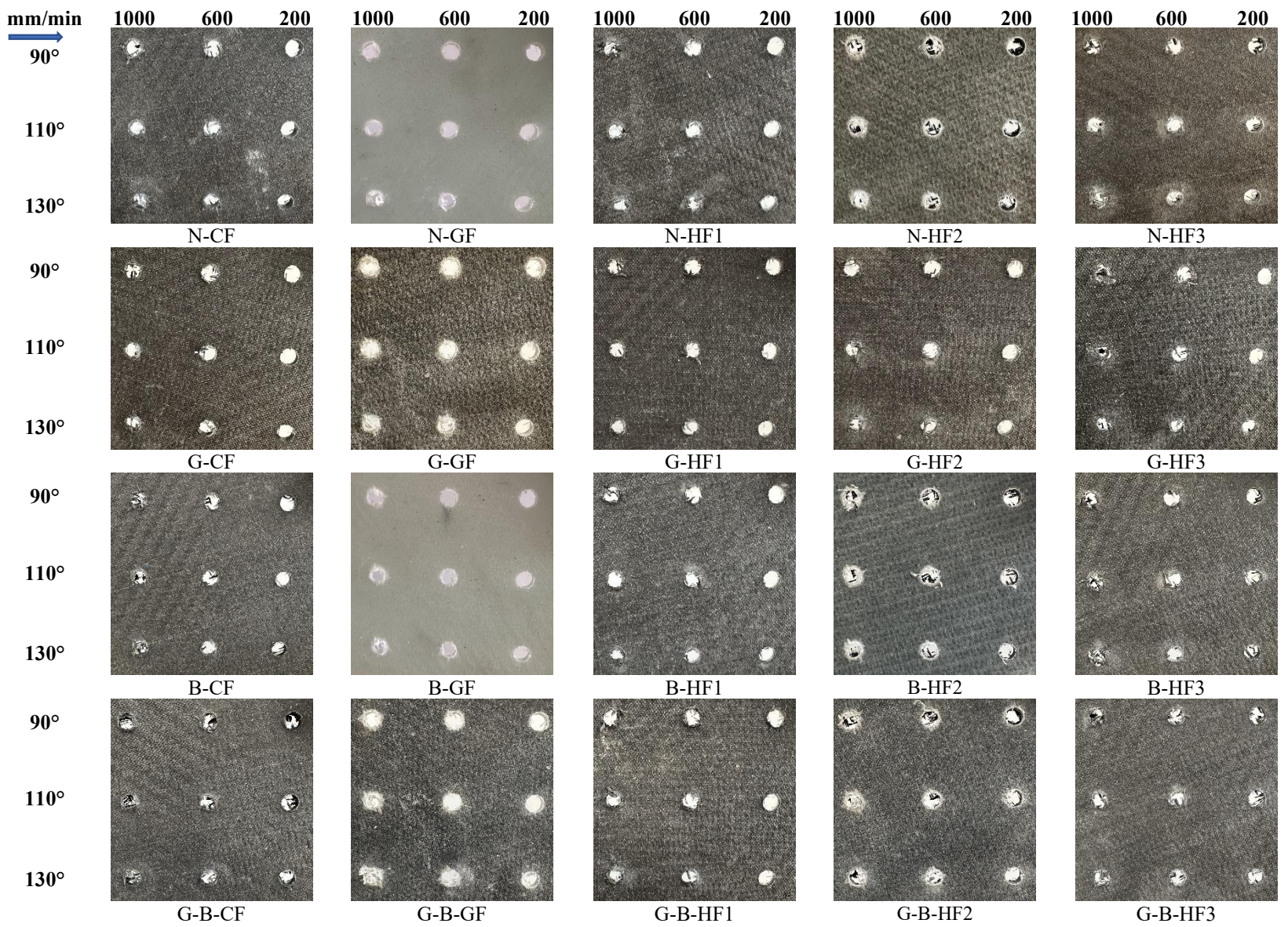


Figure 8. Post-drilling images of the holes in composite materials under different drill point angles and feed rates.

4 CONCLUSION AND SUGGESTIONS

In this study, the effects of reinforcing epoxy-based composite materials—comprising CF, GF, and HF with different stacking sequences—with GnPs and BNNPs on density, hardness, and machinability were investigated. The main findings are summarized below:

- Density measurements revealed that the incorporation of GnPs and/or BNNPs increased the overall density of the composites. The lowest density was recorded for the neat CF specimen (N-CF) at 1.29 g·cm⁻³, while the highest density was observed in the G-B-GF specimen, which contained both GnPs and BNNPs, at 1.83 g·cm⁻³. This increase was attributed to the high specific gravity of the nanoparticles and their distribution within the matrix.
- Hardness tests indicated that the addition of nanoparticles reduced the hardness due to increased ductility of the material, with BNNP-reinforced specimens showing the greatest reduction of about 15%. This decrease in hardness also correlates with the improved drilling machinability, as a more ductile matrix accommodates cutting forces better, resulting in reduced delamination and more uniform hole diameters. The highest hardness value was 114.95 HRL for the N-CF specimen, whereas the lowest value was 75.35 HRL for the B-GF specimen. It was observed that BNNPs led to a more significant increase in ductility compared to GnPs, which in turn caused a greater reduction in hardness.
- Machinability evaluations were conducted based on hole diameter, burr formation, and delamination behavior. In all conditions, the hole diameters obtained from drilling were smaller than the nominal drill diameter. The incorporation of nanoparticles improved the machinability by enhancing the ductility of the composite structure, allowing for larger hole diameters. The optimum hole diameter (Ø6.48 mm) was achieved in the B-GF specimen drilled at 130° point angle and 200 mm/min feed rate.
- Delamination and burr formation increased with higher feed rates. The most significant damage was observed when drilling was performed using a 130° drill at a feed rate of 1000 mm/min, while the minimum burr formation occurred at a feed rate of 200 mm/min. GF-based specimens (N-GF, G-GF, B-GF, G-B-GF) exhibited less delamination and burr formation compared to other specimens, which was attributed to the enhanced ductility provided by the GF reinforcement. This ductile behavior helped absorb cutting forces more effectively, thereby preserving surface integrity.

In conclusion, the addition of GnPs and BNNPs resulted in increased density, reduced hardness, and significant improvements in machinability. Among all the samples, the GF-based composites reinforced with nanoparticles demonstrated superior performance in terms of machinability. Future studies may focus on investigating the effects of different types and concentrations of nanoparticles on the drilling behavior of natural fiber composites under various environmental and thermal aging conditions.

Acknowledgements

This study was performed using some of the materials produced during the Master's thesis project of Umut Ozgur OZALTAY, supervised by Alper GUNOZ at the Institute of Science, Mersin University. The study was supported by the Mersin University Scientific Research Projects Unit under project number 2023-2-TP2-4988.

Conflict of Interest Statement

There is no conflict of interest between the authors.

Statement of Research and Publication Ethics

The study is complied with research and publication ethics.

Artificial Intelligence (AI) Contribution Statement

During the preparation of this manuscript, the authors used artificial intelligence (ChatGPT) to improve the clarity and readability of the English text. All outputs were carefully reviewed and edited by the authors, who take full responsibility for the content of this publication.

Contributions of the Authors

Alper GUNOZ: investigation; methodology; data curation; formal analysis; validation; supervision; writing – review and editing.

Umut Ozgur OZALTAY: investigation; resources; visualization; roles/writing – original draft.

REFERENCES

- [1] L. Urtekin, D. Gunes, F. Yılan, and M. Çanlı, "The effect of layers on the unidirectional carbon fibers of the reinforced polyester resin matrix composite material," *Gazi Üniversitesi Fen Bilimleri Dergisi Part C: Tasarım ve Teknoloji*, vol. 10, no. 3, pp. 495-503, 2022.
- [2] M. R. Zakaria, M. H. A. Kudus, H. M. Akil, and M. Z. M. Thirmizir, "Comparative study of graphene nanoparticle and multiwall carbon nanotube filled epoxy nanocomposites based on mechanical, thermal and dielectric properties," *Composites Part B: Engineering*, vol. 119, pp. 57-66, 2017.
- [3] İ. Bozkurt, "Numerical investigation of the effects of impactor geometry on impact behavior of sandwich structures," *Bitlis Eren Üniversitesi Fen Bilimleri Dergisi*, vol. 13, no. 3, pp. 750-771, 2024.
- [4] A. Gunoz and M. Kara, "Damage behavior of functionally graded kevlar/carbon epoxy nanocomposites reinforced with polyamide 6.6 nanofiber and MWCNTs subjected to low-velocity impact," *International Journal of Damage Mechanics*, p. 10567895241305324, 2024.
- [5] A. Gunoz and M. Kara, "Mechanical behavior of the polyamide 6.6 nanofiber and MWCNT-reinforced hybrid nanocomposites," *Polymer Composites*, vol. 45, no. 5, pp. 4693-4708, 2024.
- [6] H. Ulus, T. Üstün, Ö. S. Şahin, S. E. Karabulut, V. Eskizeybek, and A. Avcı, "Low-velocity impact behavior of carbon fiber/epoxy multiscale hybrid nanocomposites reinforced with multiwalled carbon nanotubes and boron nitride nanoplates," *Journal of Composite Materials*, vol. 50, no. 6, pp. 761-770, 2016.
- [7] H. B. Kaybal, H. Ulus, O. Demir, Ö. S. Şahin, and A. Avcı, "Effects of alumina nanoparticles on dynamic impact responses of carbon fiber reinforced epoxy matrix nanocomposites," *Engineering Science and Technology, an International Journal*, vol. 21, no. 3, pp. 399-407, 2018.
- [8] D. Lee *et al.*, "Enhanced mechanical properties of epoxy nanocomposites by mixing noncovalently functionalized boron nitride nanoflakes," *Small*, vol. 9, no. 15, pp. 2602-2610, 2013.
- [9] H. Ulus, T. Üstün, V. Eskizeybek, Ö. S. Şahin, A. Avcı, and M. Ekrem, "Boron nitride-MWCNT/epoxy hybrid nanocomposites: Preparation and mechanical properties," *Applied Surface Science*, vol. 318, pp. 37-42, 2014.
- [10] H. Sepetcioglu *et al.*, "Improved mechanical properties of graphene-modified basalt fibre–epoxy composites," *Nanotechnology Reviews*, vol. 13, no. 1, p. 20240052, 2024.
- [11] Ç. Uzay and M. S. Kamer, "Effect of Silane-Coated SiO2 Nanoparticles on the Hardness Values of Glass FRP Composites," *Bitlis Eren Üniversitesi Fen Bilimleri Dergisi*, vol. 11, no. 3, pp. 751-758, 2022.
- [12] Z. A. Oğuz, "UV aging effect on buckling properties of nanoclay particulated intraply hybrid composites," *Physica Scripta*, vol. 100, no. 2, p. 025916, 2025.
- [13] H. Geçmez and H. A. Deveci, "Optimization Of Hybrid Composite Laminates With Various Materials Using GA/GPSA Hybrid Algorithm for Maximum Dimensional Stability," *Bitlis Eren Üniversitesi Fen Bilimleri Dergisi*, vol. 13, no. 1, pp. 107-133, 2024.
- [14] K. Nagaraja, G. Rajeshkumar, M. Sanjay, and S. Siengchin, "Influence of stacking sequence and halloysite addition on the fracture toughness and low-velocity impact strength of carbon/glass fiber reinforced hybrid composites," *Polymer Composites*, vol. 45, no. 1, pp. 328-337, 2024.
- [15] F. Karaca, "Cam elyaf takviyeli plastik kompozitlerde delme parametrelerinin deformasyon faktörüne etkisinin araştırılması," *Fırat Üniversitesi Mühendislik Bilimleri Dergisi*, vol. 28, no. 2, pp. 23-27, 2016.
- [16] G. Başar, Y. Fedai, and H. K. Akın, "Kompozit malzemelerin delme işleminde itme kuvvetinin taguchi metodu ile optimizasyonu ve regresyon analizi ile tahmini," *Çukurova Üniversitesi Mühendislik-Mimarlık Fakültesi Dergisi*, vol. 35, no. 4, pp. 969-982, 2020.
- [17] H. Ho-Cheng and C. Dharan, "Delamination during drilling in composite laminates," *Journal of Manufacturing Science and Engineering*, vol. 112, no. 3, pp. 236-239, 1990.
- [18] T. Rajamurugan, K. Shanmugam, and K. Palanikumar, "Analysis of delamination in drilling glass fiber reinforced polyester composites," *Materials & Design*, vol. 45, pp. 80-87, 2013.
- [19] T. Sunny, J. Babu, and J. Philip, "Experimental studies on effect of process parameters on delamination in drilling GFRP composites using Taguchi method," *Procedia Materials Science*, vol. 6, pp. 1131-1142, 2014.

- [20] J. Matuszak and K. Zaleski, "Edge states after wire brushing of magnesium alloys," *Aircraft Engineering and Aerospace Technology: An International Journal*, vol. 86, no. 4, pp. 328-335, 2014.
- [21] J. Matuszak and K. Zaleski, "Analysis of deburring effectiveness and surface layer properties around edges of workpieces made of 7075 aluminium alloy," *Aircraft Engineering and Aerospace Technology*, vol. 90, no. 3, pp. 515-523, 2018.
- [22] J. Matuszak, M. Kłonica, and I. Zagórski, "Measurements of forces and selected surface layer properties of AW-7075 aluminum alloy used in the aviation industry after abrasive machining," *Materials*, vol. 12, no. 22, p. 3707, 2019.
- [23] C. Tsao, H. Hocheng, and Y. Chen, "Delamination reduction in drilling composite materials by active backup force," *CIRP annals*, vol. 61, no. 1, pp. 91-94, 2012.
- [24] N. Anaç *et al.*, "Cam fiber takviyeli plastik malzemelerin delaminasyon durumunun incelenmesi," *Mühendislik Bilimleri ve Tasarım Dergisi*, vol. 13, no. 1, pp. 234-249, 2025.
- [25] E. Unal, "Temperature and thrust force analysis on drilling of glass fiber reinforced plastics," *Thermal Science*, vol. 23, no. 1, pp. 347-352, 2019.
- [26] V. K. Vankanti and V. Ganta, "Optimization of process parameters in drilling of GFRP composite using Taguchi method," *Journal of Materials Research and Technology*, vol. 3, no. 1, pp. 35-41, 2014.
- [27] L. Gemi, S. Morkavuk, U. Köklü, and D. S. Gemi, "An experimental study on the effects of various drill types on drilling performance of GFRP composite pipes and damage formation," *Composites Part B: Engineering*, vol. 172, pp. 186-194, 2019.
- [28] K. K. Singh and D. Kumar, "Experimental investigation and modelling of drilling on multi-wall carbon nanotube–embedded epoxy/glass fabric polymeric nanocomposites," *Proceedings of the Institution of Mechanical Engineers, Part B: Journal of Engineering Manufacture*, vol. 232, no. 11, pp. 1943-1959, 2018.
- [29] H. Heidary, N. Z. Karimi, and G. Minak, "Investigation on delamination and flexural properties in drilling of carbon nanotube/polymer composites," *Composite Structures*, vol. 201, pp. 112-120, 2018.
- [30] T. Sathish and B. Varadhan, "Enhancing drilling performance in hybrid Basalt/E-Glass fiber epoxy modified with MWCNTs+SiO2 nanocomposites," *The International Journal of Advanced Manufacturing Technology*, vol. 136, no. 1, pp. 315-328, 2025.
- [31] F. Erhan, L. Gemi, Ş. Yazman, S. Morkavuk, and U. Köklü, "A comprehensive investigation into the influence of variation in the stacking sequence on the mechanical behaviour and drilling machinability of basalt fiber-reinforced composite tubes," *Composites Part B: Engineering*, vol. 299, p. 112405, 2025.
- [32] N. Patel, K. Patel, V. Chaudhary, and P. Gohil, "Investigations on drilling of hybrid basalt/glass polyester composites," *Australian Journal of Mechanical Engineering*, vol. 20, no. 4, pp. 1154-1163, 2022.
- [33] L. Gemi, U. Köklü, Ş. Yazman, and S. Morkavuk, "The effects of stacking sequence on drilling machinability of filament wound hybrid composite pipes: Part-1 mechanical characterization and drilling tests," *Composites Part B: Engineering*, vol. 186, p. 107787, 2020.
- [34] H. Sepetcioglu, A. Gunoz, and M. Kara, "Effect of hydrothermal ageing on the mechanical behaviour of graphene nanoplatelets reinforced basalt fibre epoxy composite pipes," *Polymers and Polymer Composites*, vol. 29, no. 9_suppl, pp. S166-S177, 2021.
- [35] K. A. Zarasvand and H. Golestanian, "Investigating the effects of number and distribution of GNP layers on graphene reinforced polymer properties: Physical, numerical and micromechanical methods," *Composites Science and Technology*, vol. 139, pp. 117-126, 2017.
- [36] J. Naveen, M. Jawaid, E. S. Zainudin, M. Thariq Hameed Sultan, and R. Yahaya, "Improved mechanical and moisture-resistant properties of woven hybrid epoxy composites by graphene nanoplatelets (GNP)," *Materials*, vol. 12, no. 8, p. 1249, 2019.
- [37] T. Üstün *et al.*, "Evaluating the effectiveness of nanofillers in filament wound carbon/epoxy multiscale composite pipes," *Composites Part B: Engineering*, vol. 96, pp. 1-6, 2016.
- [38] ASTM D792-20: Standard test methods for density and specific gravity (relative density) of plastics by displacement, ASTM, West Conshohocken, PA, USA, 2013.
- [39] ASTM D785-08: Standard Test Method for Rockwell Hardness of Plastics and Electrical Insulating Materials, ASTM, West Conshohocken, PA, USA, 2015.

- [40] M. A. Doğan, Ş. Yazman, L. Gemi, M. Yildiz, and A. Yapici, "A review on drilling of FML stacks with conventional and unconventional processing methods under different conditions," *Composite Structures*, vol. 297, p. 115913, 2022.
- [41] Ş. Yazman, L. Gemi, S. Morkavuk, and U. Köklü, "Investigation of the effect of symmetrical hybrid stacking on drilling machinability of unidirectional CFRP, GFRP and hybrid composites: Drilling tests and damage analysis," *Composites Part A: Applied Science and Manufacturing*, vol. 187, p. 108486, 2024.
- [42] F. Ceritbinmez and A. Yapıcı, "Kompozit malzemelerin delinmesinde matkap nokta açısının ve ÇCKNT'lerin etkisi," *Academic Perspective Procedia*, vol. 3, no. 1, pp. 180-188, 2020.
- [43] G. Franz, P. Vantomme, and M. H. Hassan, "A review on drilling of multilayer fiber-reinforced polymer composites and aluminum stacks: optimization of strategies for improving the drilling performance of aerospace assemblies," *Fibers*, vol. 10, no. 9, p. 78, 2022.
- [44] D. Liu, Y. Tang, and W. Cong, "A review of mechanical drilling for composite laminates," *Composite Structures*, vol. 94, no. 4, pp. 1265-1279, 2012.
- [45] M. Mehdikhani, L. Gorbatikh, I. Verpoest, and S. V. Lomov, "Voids in fiber-reinforced polymer composites: A review on their formation, characteristics, and effects on mechanical performance," *Journal of Composite Materials*, vol. 53, no. 12, pp. 1579-1669, 2019.
- [46] P. Govindaraj *et al.*, "Distribution states of graphene in polymer nanocomposites: A review," *Composites Part B: Engineering*, vol. 226, p. 109353, 2021.
- [47] M. Owais, J. Zhao, A. Imani, G. Wang, H. Zhang, and Z. Zhang, "Synergetic effect of hybrid fillers of boron nitride, graphene nanoplatelets, and short carbon fibers for enhanced thermal conductivity and electrical resistivity of epoxy nanocomposites," *Composites Part A: Applied Science and Manufacturing*, vol. 117, pp. 11-22, 2019.
- [48] X. Jiang, M. Gao, J. Zhu, H. Ji, and F. Lang, "Studying the interfacial properties of carbon/glass hybrid composites via the nanoindentation method," *Polymers*, vol. 14, no. 14, p. 2897, 2022.
- [49] A. Caggiano, "Machining of fibre reinforced plastic composite materials," *Materials*, vol. 11, no. 3, p. 442, 2018.
- [50] J. P. Davim, Machinability of fibre-reinforced plastics. Walter de Gruyter, 2015.
- [51] M. T. H. Sultan, A. I. Azmi, M. S. Abd Majid, M. R. M. Jamir, and N. Saba, *Machining and Machinability of Fiber Reinforced Polymer Composites*. Springer, 2020.
- [52] A. P. Mouritz, *Introduction to aerospace materials*. Elsevier, 2012.
- [53] F. Shi, Y. Yang, N. Sun, Z. Du, C. Zhang, and D. Zhao, "Research on Damage Caused by Carbon-Fiber-Reinforced Polymer Robotic Drilling Based on Digital Image Correlation and Industrial Computed Tomography," *Machines*, vol. 12, no. 1, p. 22, 2023.
- [54] H. B. Kaybal, A. Unuvar, Y. Kaynak, and A. Avcı, "Evaluation of boron nitride nanoparticles on delamination in drilling carbon fiber epoxy nanocomposite materials," *Journal of Composite Materials*, vol. 54, no. 2, pp. 215-227, 2020.
- [55] R. K. Thakur and K. K. Singh, "Evaluation of drilling characteristics to explore the effect of graphene nanoplatelets on glass fiber reinforced polymer composite," *Measurement*, vol. 219, p. 113233, 2023.
- [56] R. K. Thakur, K. K. Singh, and P. Rawat, "Evaluation of graphene nanoplatelets addition and machining methods on the hole quality and bearing strength of glass and carbon fibre reinforced epoxy laminates," *Journal of Manufacturing Processes*, vol. 115, pp. 137-155, 2024.
- [57] J. P. Davim and P. Reis, "Drilling carbon fiber reinforced plastics manufactured by autoclave—experimental and statistical study," *Materials & design*, vol. 24, no. 5, pp. 315-324, 2003.
- [58] J. P. Davim, P. Reis, and C. C. António, "Experimental study of drilling glass fiber reinforced plastics (GFRP) manufactured by hand lay-up," *Composites Science and Technology*, vol. 64, no. 2, pp. 289-297, 2004.